frontiers | Frontiers in Environmental Science

TYPE Original Research
PUBLISHED 04 September 2025
DOI 10.3389/fenvs.2025.1626677

OPEN ACCESS

EDITED BY
Giuseppe Mancuso,
University of Bologna, Italy

REVIEWED BY
Ayman Youssef I. Ewida,
National Water Research Center (NWRC), Egypt
Halil Ibrahim Burgan,
Akdeniz University, Türkiye

*CORRESPONDENCE
Long Yang,
yanglong@cidp.edu.cn

RECEIVED 11 May 2025
ACCEPTED 21 July 2025
PUBLISHED 04 September 2025

CITATION
Yang L, Ou Y and Yao Y (2025) Research on estimating the nitrogen pollutant load of agricultural drainage water in the Ningxia irrigation area based on the improved ECM model.
Front. Environ. Sci. 13:1626677.
doi: 10.3389/fenvs.2025.1626677

Research on estimating the nitrogen pollutant load of agricultural drainage water in the Ningxia irrigation area based on the improved ECM model

Long Yang[1,2]*, Yang Ou[3] and Yao Yao[1,2]

[1]School of Environment and Disaster Management, Institute of Disaster Prevention, Sanhe, China, [2]Hebei Key Laboratory of Resource and Environmental Disaster Mechanism and Risk Monitoring, Sanhe, China, [3]State Key Laboratory of Black Soils Conservation and Utilization, Northeast Institute of Geography and Agroecology, Chinese Academy of Sciences, Changchun, China

Agricultural drainage water pollution in Ningxia irrigation areas is a significant factor affecting water quality in the Yellow River Basin. Based on the principle of total nitrogen (TN) input–output conservation, and incorporating irrigation and precipitation correction factors, an improved Export Coefficient Model (ECM) was developed to estimate the TN pollution load from agricultural drainage water. The spatiotemporal distribution characteristics of TN pollution load in Ningxia irrigation districts were analyzed, leading to the following conclusions: 1) from 2010 to 2022, the annual TN export coefficient and multi-year average total load from agricultural drainage water in Ningxia irrigation areas were 26.85 kg/ha·a^{-1} and 2064.95 t/a, respectively, showing a significant downward trend overall; 2) major changes in the crop structure occurred in Ningxia irrigation areas between 2010 and 2022, with a sharp decline in the rice planting area being the primary factor reducing the pollution load; 3) the spatial distribution of TN pollution load in 2010, 2015, and 2022 exhibited significant heterogeneity, allowing division into high-pollution, medium-pollution, and low-pollution zones. High-pollution zones were primarily located in Pingluo County, Qingtongxia City, and Zhongning County. The improved ECM more accurately reflects actual conditions compared to its predecessor and can support the estimation of agricultural return flow pollution loads in irrigation districts and the management of non-point source pollution in river basins.

KEYWORDS

pollutant load, TN, ECM model, agricultural drainage water, Ningxia irrigation district

1 Introduction

The discharge from irrigation districts carries pollutants such as nitrogen and phosphorus, which are not absorbed by crops, into water bodies, posing a threat to the water quality of receiving water bodies. As one of the sources of non-point source pollution (NPSP) in aquatic environments, it is influenced by multiple factors including land use patterns, fertilization intensity, irrigation water volume, climate change, and soil properties (Lu et al., 2024; Meng-bing et al., 2025). This type of pollution is characterized by difficulties in monitoring and irregular discharge patterns. In recent years, scholars have integrated

NPSP loads into water environment system management research, providing theoretical references for assessing pollution loads from agricultural drainage water.

1.1 Principles and applications of the ECM

The estimation of water load in farmland drainage water generally requires the use of physical process models and export coefficient models (ECM). The refinement and localization of physical process models have emerged as key research directions. For instance, the Soil and Water Assessment Tool (SWAT) model is widely applied in simulating return flow pollution in irrigation districts, yet it faces limitations in characterizing unique hydrological processes under constrained information conditions (Zhang et al., 2024; Yuanzhe et al., 2023). However, factors such as complex NPSP mechanisms, intensive computational demands, and numerous parameters hinder the practical application of distributed physical process models. Consequently, scholars have proposed simplified methods for pollution load estimation (e.g., average concentration method, hydrological estimation method, and unit load method), which are now extensively adopted in NPSP studies (Chaofan et al., 2020; Li et al., 2018; Geng et al., 2013). The ECM, also termed the "unit area load method," originated in North America (e.g., USA and Canada) during the late 1960s to early 1970s through studies on the "land use-nutrient load-eutrophication" relationship (Girolamo et al., 2019; Stephan and Endreny, 2016). Early ECMs primarily classified pollution sources by land use type but overlooked driving forces behind NPSP loads.

The ECM estimates regional nitrogen (TN) and phosphorus (TP) loss by correlating the intensity of pollution sources (such as fertilizer application and livestock and poultry breeding) with output loads and then analyzes the spatiotemporal distribution characteristics of pollution loads and source apportionment. Meng Xiaojun et al. employed the ECM to estimate the TN and TP pollution loads from agricultural non-point sources across 11 prefectures and districts in Shanxi Province for the period 2010–2019. The study aimed to clarify the spatiotemporal distribution characteristics, identify key pollution sources, determine polluted areas, and classify pollution types within these regions (Meng et al., 2024). Gou Ting et al. (2020) applied an improved version of the ECM to analyze the characteristics of nitrogen and phosphorus emissions from agricultural non-point sources in the Dongjiang River source region. Their findings revealed that the annual average TN and TP pollution loads in the Dongjiang River source area were 4,884.23 t/a and 591.85 t/a, respectively. The study further indicated variations in nitrogen and phosphorus load intensities, with distinct spatial patterns observed. Additionally, the contribution rates of different pollution sources to nitrogen and phosphorus emissions differed significantly. Specifically, TN emissions were primarily attributed to land use, followed by rural domestic activities and livestock and poultry breeding. In contrast, TP emissions were predominantly driven by livestock and poultry breeding, followed by land use and rural domestic activities (Gou et al., 2023).

1.2 ECM model improvement and optimization strategies

To enhance the simulation accuracy of complex terrain areas, some scholars have introduced correction factors such as rainfall influence and terrain slope to improve the model. He Yun et al. introduced rainfall and terrain factors (α,β) to study the classical ECM. Compared with the actual observed values, the average relative deviations of the estimated values of TN and TP loads of the improved ECM were 9.80% and 2.09%, respectively. Compared with the model before improvement, it can more accurately estimate the agricultural non-point source pollution in the Beipanjiang River Basin (Qinglong section) in the southwest karst mountainous area, providing a reference for NPSP load estimation in the karst mountainous area (He et al., 2022). Hu Zheng et al. incorporated rainfall and topography for enhancing the ECM, estimating agricultural TN and TP (total phosphorus) loads in the Quxian watershed. Results showed annual outputs of 503.84 t TN and 53.85 t TP, with relative errors of 10.87% (TN) and 13.86% (TP), validating the model's reliability (Hu et al., 2019). Yang Shujing et al. improved the ECM by introducing irrigation impact factor and estimated the agricultural non-point source pollutant loads in the Ningxia irrigation area by the improved model. Compared with the traditional models, the relative error of the TN load estimate results from the improved model decreased by 5%, and that of the TP load estimate results decreased by 13%. The calculation results obtained from the improved model were closer to those of the actual pollution situation of the irrigation area than the traditional ECMs (Yang et al., 2009).

1.3 Integration of ECMs with new technologies

In recent years, with the development of new technologies, by coupling 3S, other models, intelligent monitoring, and other technologies, the progress of data sources for ECMs has been improved, the accuracy of multi-source data analysis of ECMs has been enhanced, and the spatial distribution of pollution loads has been visually analyzed to identify priority control areas. To clarify the current situation of agricultural non-point source pollution and identify the main sources and regions in Hebei Province, Li Tongtong et al. evaluated its load from 2000 to 2021 using the ECM and conducted spatiotemporal characteristic analysis using GIS. The results show that the environmental impact of agricultural non-point source pollution in the southwestern region of Hebei Province is significantly more serious than that in the northeastern region. The emissions of agricultural non-point source pollution showed significant downward inflection points in 2007 and 2017, respectively, reaching the lowest value in 2021 (Li et al., 2024). Chen Haiyang et al. selected the Jinjiang area as an example and proposed the comprehensive application of the runoff process SLURP model based on semi-distributed land use, the ECM, and the modified General Soil Loss Equation (RUSLE) for the load estimation and source allocation of nitrogen and phosphorus (Haiyang et al., 2013). Accurate pollution export coefficients are crucial for reducing uncertainties in load estimation. By integrating artificial simulated rainfall experiments with field survey data, R. Liu

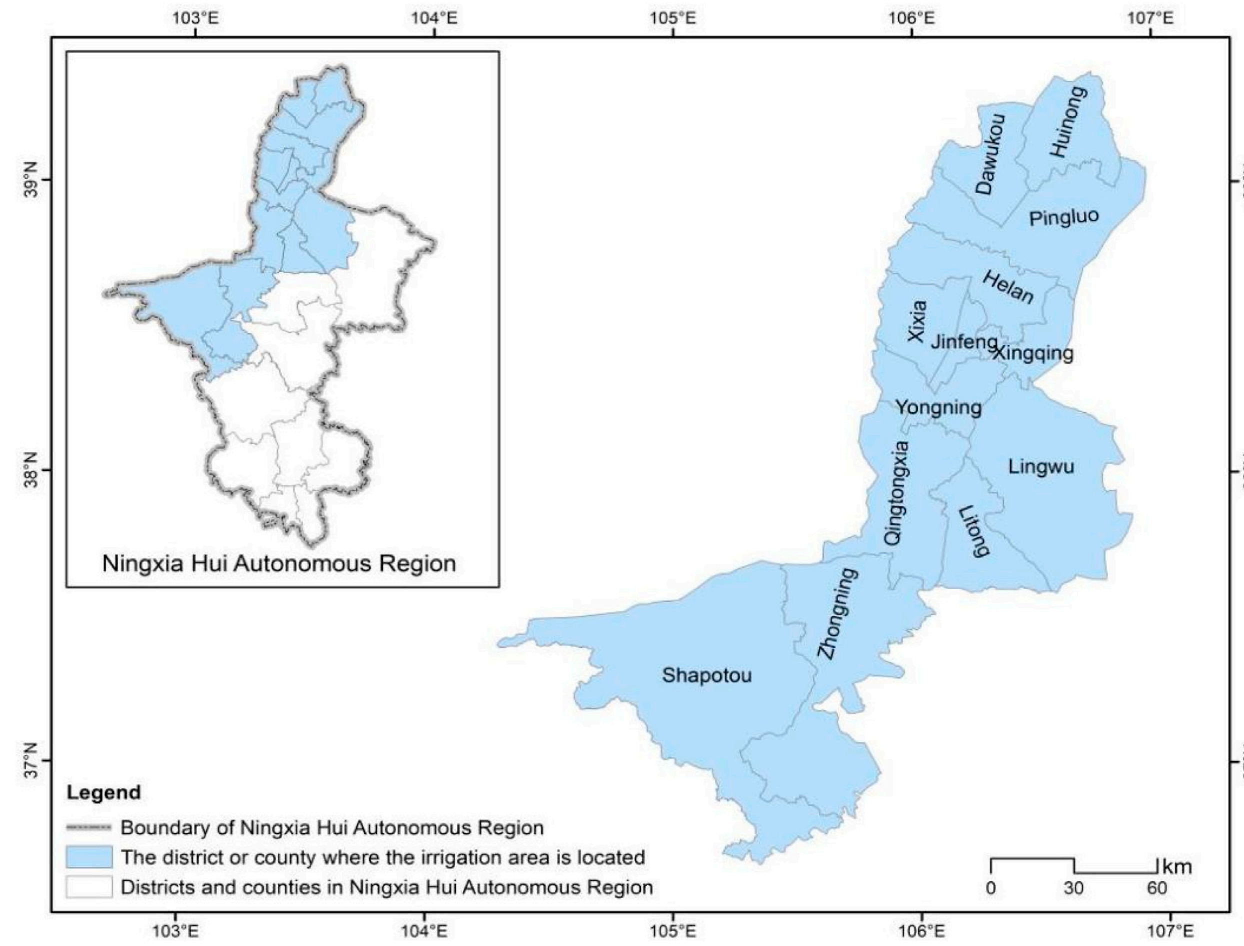

FIGURE 1
Location map of the study area.

et al. have developed a new method that estimates regional pollution export coefficients. Results showed that the export coefficients calculated accurately express the regional rainfall–runoff characteristics as the simulation precision of this method had increased by 30% compared to the results with traditional ECM and export coefficients, surveyed from the literature (Liu et al., 2017). The Diffuse Pollution Estimation with Remote Sensing (DPeRS) model, a distributed NPSP model proposed by Chinese researchers, seeks to predict agricultural NPSP and includes modules estimating nitrogen and phosphorus balance, vegetation coverage, dissolved pollution, and absorbed pollution (Chen et al., 2025).

In summary, the improved ECM incorporates more rational factors, requiring fewer parameters, offering simpler operation, and delivering higher precision. It is particularly suitable for estimating non-point source pollution loads in large and medium-sized river basins with insufficient hydrological and water quality monitoring data and research foundations are relatively weak (HuaLin et al., 2023; Xiaoyuan et al., 2023). In the Ningxia irrigation district, the lack of long-term effective monitoring of agricultural drainage water, coupled with significant variations in rainfall and irrigation conditions, necessitates scientific assessment of pollution loads under data constraints to better support regional water environment management. This study considers the influencing factors of rainfall and irrigation, enhancing the ECM through irrigation and rainfall factors based on mass input conservation. It estimates the TN pollution load in agricultural drainage water within the Ningxia irrigation district and subsequently analyzes the spatiotemporal characteristics of TN pollution export from farmland drainage in the irrigated area.

2 Materials and methods

2.1 Overview of the area to be researched

The Ningxia irrigation area is one of the four ancient irrigation areas in China. It is located along the Yellow River in northern Ningxia. It has an irrigation history of more than 2,000 years. The irrigation area is distributed in a "J"-shaped belt on both sides of the Yellow River. The land in the irrigation area accounts for 41% of the whole land area of Ningxia, but it provides approximately 70% of the food for whole Ningxia. Divided by Qingtongxia Water Conservancy Project, the Ningxia irrigation area includes the Weining irrigation area upstream and Qingtongxia irrigation area

TABLE 1 Basic situation of agricultural irrigation water in Ningxia.

Year	Water withdrawal per unit area (m^3/ha)	Agricultural irrigation area (10^4 ha)	Irrigation efficiency coefficient	Irrigation water volume (100 million m^3)	Water discharge volume into the Yellow River (100 million m^3)
2010	765	868.00	0.493	66.402	33.189
2011	788	850.00	0.485	66.980	34.008
2012	778	802.45	0.460	62.431	33.456
2013	795	818.11	0.482	65.040	33.367
2014	709	859.83	0.475	60.962	31.449
2015	705	873.19	0.501	61.560	31.048
2016	636	879.70	0.511	55.949	28.516
2017	625	901.70	0.524	56.356	29.072
2018	627	897.20	0.535	56.254	27.059
2019	648	912.31	0.543	59.118	25.979
2020	591	983.60	0.551	58.131	24.790
2021	532	1046.4	0.561	55.668	22.712
2022	524	1057.44	0.570	55.410	20.318
2023	515	1075.00	0.579	55.363	17.193

downstream (Liu et al., 2025). The location of the study area is shown in Figure 1. The agricultural sector in Ningxia's irrigation area features diversified crop cultivation, with staple grains including rice, wheat, and corn. Specialty agriculture has experienced rapid development, particularly in the expanding cultivation of goji berries and grapes. Farmland fertilizer input across various cities and counties in the irrigation area remains consistently high, resulting in substantial nitrogen and phosphorus surpluses that inevitably contribute to nutrient runoff into water bodies. The practice of flood irrigation in rice paddies generates agricultural drainage water, which constitutes one of the primary factors affecting water quality in the middle and upper reaches of the Yellow River (Pei et al., 2024).

Based on the needs of crop growth and the law of agricultural activities, the period for agricultural irrigation in Ningxia is divided into spring–summer irrigation period and winter irrigation period. The spring–summer irrigation starts from late April and ends in mid- or late September, and the winter irrigation starts from late October and ends in mid-November. The annual irrigation period is approximately 180 days. The drainage system in Ningxia irrigation area is well developed, and there are 32 main drainage ditches mainly used for agricultural irrigation. The agricultural irrigation situation in Ningxia, based on the 2010–2023 Ningxia Water Resources Bulletin, is shown in Table 1.

2.2 Selection and improvement of the ECM

According to the conservation of matter, the input and export balance of elements in nature is considered in the definition of the export coefficient. The input pathways of TN include application of nitrogen fertilizer, dry/wet deposition, and plant nitrogen fixation; the export pathways of TN mainly include crop absorption, ammonia nitrogen volatilization, infiltration, and surface rainfall runoff loss. The export–input equilibrium equation of TN is established as follows:

$$I_1+I_2+I_3 = O_1+O_2+O_3 + O_4 \quad (1)$$

where I_1: annual input of pure nitrogen (converted from nitrogen fertilizer) per unit area of the planting land, kg/ha·a^{-1}; I_2: annual dry/wet nitrogen deposition per unit area of the planting land, kg/ha·a^{-1}; I_3: annual plant nitrogen fixation per unit area, kg/ha·a^{-1}; O_1: annual nitrogen absorption of crops per unit area, kg/ha·a^{-1}; O_2: amount of volatile nitrogen per unit area of the planting land, kg/ha·a^{-1}; O_3: amount of nitrogen infiltrated into groundwater per unit area per year, kg/ha·a^{-1}; O_4: annual total nitrogen runoff loss per unit area, kg/ha·a^{-1}.

Based on the export–input equilibrium equation, the expression of the TN export coefficient (E_{NA}) of agricultural drainage water in the irrigation area can be obtained:

$$E_{NA} = O_4 = I_1+I_2+I_3 - O_1 - O_2 - O_3 \quad (2)$$

To facilitate the follow-up study and calculation of agricultural drainage water, the difference between deposition term I_2 and volatile term O_2 is recorded as E_2, representing the net settlement value. Based on the export–input equilibrium equation, the expression of the total nitrogen export coefficient of farmland planting can be obtained:

$$E_{NA} = O_4 = I_1+I_3+E_2 - O_1 - O_3 \quad (3)$$

Considering the impact of driving forces on non-point source pollution loads, researchers often improve models by

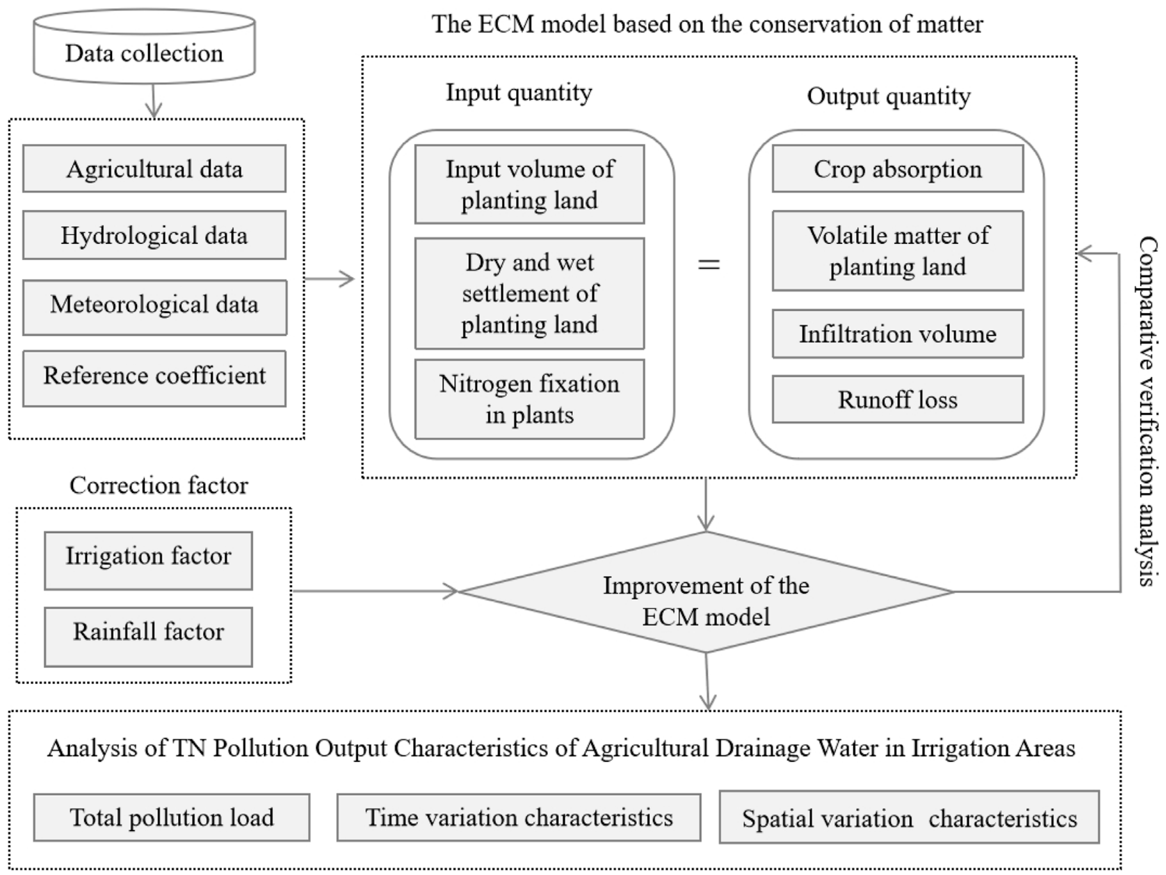

FIGURE 2
Technical roadmap.

incorporating factors such as irrigation correction factors, precipitation correction factors, and topographic influence factors, thereby making simulation estimates more accurate (Lu et al., 2012). The amount of water withdrawal from farmland directly affects the strength of pollutant sources in farmland irrigation areas. Zhao Xinyu analyzed the irrigation amount and water withdrawal in the Qingtongxia irrigation area, Ningxia, and found that the water withdrawal increased with the increase in the irrigation amount with a strong correlation between them (correlation coefficient: 0.73) (Xinyu et al., 2007). With high levels of irrigation, the surface water on paddy fields will overflow over the ridges or infiltrate laterally, increasing the amount of water withdrawn. Additionally, the amount of pesticides, fertilizers, and other pollutants carried by water withdrawal will also increase. Once the water withdrawn is discharged into rivers, it will affect the water quality of the receiving river bodies. Therefore, irrigation intensity affects the specific TN and TP loads in the water bodies receiving the agricultural drainage water. Both amount and intensity of precipitation directly affect the export of non-point source pollution, and there is a good correlation between non-point source pollution and runoff in the watershed (Li et al., 2025). It is seen that adding the precipitation factor to the ECM can help it more accurately estimate the nitrogen and phosphorus pollutant loads. Considering that the Ningxia irrigation area is located in the plain area and the agricultural drainage water mainly comes from paddy fields, irrigation impact factor and precipitation impact factor are used as model improvement inputs in this research. The improved ECM is shown in Equation 4. The technical route is shown in Figure 2.

$$L = \alpha\beta\sum_{i=1}^{n} A_{NAi} \cdot E_{NAi} \tag{4}$$

where L represents the output load of the pollutant, kg; α represents the irrigation impact factor; β represents the precipitation impact factor; A_{NAi} represents the farmland planting area in the ith area, ha; and E_{NAi} represents the TN export coefficient of farmland planting in the ith area, kg/ha·a^{-1}.

2.3 Fundamental data acquisition

In this research, the data of precipitation, sown area, and yield of rice, use of nitrogen and phosphate fertilizers in the farmland in Ningxia irrigation area were obtained by referring to Ningxia Statistical Yearbook and Water Resources Bulletin and by field investigation. In addition, the basic data of agricultural production and hydrological data in Ningxia irrigation area were collected. The correlation coefficients were mainly sourced from the references.

TABLE 2 Annual pure nitrogen input per unit area of the cultivated land in the Ningxia irrigation district (unit: kg/ha·a^{-1}).

County/City		2010	2011	2012	2013	2014	2015	2016	2017	2018	2019	2020	2021	2022
Yinchuan city	Yinchuan City	364.14	380.71	382.17	440.50	460.09	426.58	442.48	485.59	346.15	368.39	398.35	280.08	270.06
	Yongning County	263.71	262.46	254.95	274.37	255.15	252.38	237.37	268.05	225.01	222.53	197.50	192.97	203.74
	Helan County	301.39	297.29	293.54	324.64	275.55	248.72	232.53	258.00	250.14	253.72	231.87	213.36	210.22
	Lingwu City	259.99	254.22	269.47	315.67	323.28	336.83	342.90	293.17	239.43	243.51	228.08	237.31	243.38
Shizuishan city	Shizuishan City	415.74	409.86	351.34	339.42	318.90	335.79	307.82	349.87	304.24	295.82	278.86	267.17	238.72
	Pingluo County	313.77	313.83	383.96	398.37	406.49	355.48	414.92	422.42	395.25	415.04	406.07	396.08	356.25
Wuzhong city	Litong District	345.15	345.36	336.62	322.22	302.31	290.08	216.69	242.93	264.40	269.76	262.36	268.64	253.47
	Qingtongxia City	370.97	389.47	408.31	406.84	357.57	327.66	314.82	360.52	342.89	341.44	330.63	309.49	286.32
Zhongwei city	Shapotou District	169.51	156.02	132.46	136.99	138.86	137.77	130.85	136.45	126.38	142.21	142.12	136.85	159.03
	Zhongning County	311.34	310.50	280.07	295.63	292.57	290.41	306.19	399.71	374.27	349.57	332.35	358.74	334.81
Average		311.57	311.97	309.29	325.47	313.08	300.17	294.66	321.67	286.82	290.20	280.82	266.07	255.60

3 Results and discussion

3.1 Estimate of agricultural drainage water pollutant load in the irrigation area

3.1.1 Annual input of pure nitrogen (nitrogen fertilizer converted to pure nitrogen) per unit area of the planting land (I_1)

According to the data of agricultural fertilizer application amount and crop sown area recorded in Ningxia Statistical Yearbook, the annual input of pure nitrogen per unit area of the planting land in the Ningxia irrigation area is calculated and weighted. At present, the relevant information does not include the relevant situation and detailed data on organic fertilizer application. In addition, according to the field investigation, chemical fertilizer is mainly applied during the planting season of major crops such as rice, wheat, and corn in the Ningxia irrigation area. Therefore, the contribution of nitrogen in organic fertilizers is not considered in this calculation. In addition, arious nitrogen fertilizers are applied. According to the literature review, the average purity conversion ratio of nitrogen content in fertilizers is taken as 20% (Jia, 2024). Based on calculations, the annual pure nitrogen input per unit area of cultivated land in the Ningxia irrigation district decreased from 311.57 kg/ha/yr in 2010 to 255.60 kg/ha/yr in 2022, showing an overall downward trend, as detailed in Table 2.

3.1.2 Wet/dry N deposition (I_2) and N volatile amount (O_2) of the planting land per unit area

Dry/wet N deposition and N volatile per unit area of the planting land need to be measured dynamically for many years. Due to the lack of relevant monitoring data in the Ningxia irrigation area, they are obtained by consulting relevant literature. Liang Ting et al. monitored the input of dry/wet deposition at the five monitoring points in the four ecological regions of Shaanxi Province to explore the temporal–spatial variation of atmospheric nitrogen dry/wet deposition. The results showed that the TN dry/wet deposition in Yulin, Luochuan, Xi 'an, Yangling, and Ankang regions was 4.7 kg/ha·a^{-1}, 11.9 kg/ha·a^{-1}, 25.8 kg/ha·a^{-1}, 31.9 kg/ha·a^{-1}, and 19.2 kg/ha·a^{-1} respectively, with an average value of 18.7 kg/ha·a^{-1} during the monitoring period (Liang et al., 2014). From June 2016 to May 2018, Liang Yayu conducted a 2-year test on nitrogen dry/wet deposition in Dongyang and Yangqu, suburbs of Taiyuan City, Shanxi Province by using rain gauge, automatic precipitation and dust sampler, and Delta system. The monitoring results showed that the annual total deposition in Dongyang and Hecun was 12.9 kg/ha·a^{-1} and 15.8 kg/ha·a^{-1} respectively (Liang et al., 2019). Considering the similarity between the Ningxia irrigation area and the above areas, the N load of dry/wet deposition into the farmland in the Ningxia irrigation area is selected to be 15.8 kg/ha·a^{-1}.

According to statistics, approximately 54 × 10^6 tons of ammonia nitrogen enter the Earth's atmosphere annually through various pathways. The majority (approximately 93%) returns to terrestrial surfaces via dry and wet deposition—thus calculated as roughly 50 × 10^6 tons. Additionally, lightning contributes approximately 4.35 × 10^6 tons of ammonia nitrogen to the Earth each year (Schlesinger and Bernhardt, 2013). Based on the total nitrogen balance process in farmland, the net annual deposition flux E_2 is estimated at 0.10 kg/ha·a^{-1}.

3.1.3 Annual nitrogen fixation per unit area of planting land (I_3)

Biological nitrogen fixation refers to the process in which nitrogen-fixing microorganisms reduce nitrogen in the atmosphere to ammonia in the soil through fixation by roots. Biological nitrogen fixation plays a very important role in agricultural production. Plants absorb and utilize nitrogen from the atmosphere through nitrogen fixation, among which biological nitrogen fixation plays a major role. Therefore, biological nitrogen fixation accounts for a certain proportion of the total annual TN

TABLE 3 Nitrogen absorption of the planting land in irrigation districts (O_1).

Year	Unit yield of grain (rice)/kg/ha·a^{-1}	Basic soil fertility data/kg/ha·a^{-1}	Yield increase because of fertilization/kg/ha·a^{-1}	Grain nitrogen content ratio	stem/grain nitrogen content ratio	O_1 /kg/ha·a^{-1}
2010	8,416	4,167	4,249	0.0369	0.5329	240.34
2011	8,429	4,167	4,262	0.0369	0.5329	241.08
2012	8,457	4,167	4,290	0.0369	0.5329	242.66
2013	8,387	4,167	4,220	0.0369	0.5329	238.70
2014	7,923	4,167	3,756	0.0369	0.5329	212.45
2015	8,172	4,167	4,005	0.0369	0.5329	226.54
2016	8,394	4,167	4,227	0.0369	0.5329	239.10
2017	8,491	4,167	4,324	0.0369	0.5329	244.58
2018	8,531	4,167	4,364	0.0369	0.5329	246.85
2019	8,095	4,167	3,928	0.0369	0.5329	222.18
2020	8,122	4,167	3,955	0.0369	0.5329	223.71
2021	8,064	4,167	3,897	0.0369	0.5329	220.43
2022	8,053	4,167	3,886	0.0369	0.5329	219.81

input of planting land. Nitrogen fixation varies greatly with different crop species. Wang Xin conducted systematic sampling on paddy soil and estimated the rate of biological nitrogen fixation in the paddy soil in Yixing City by using the acetylene reduction method. The research found that the biological nitrogen fixation per unit area of paddy surface soil in Yixing City was 0.75 kg/ha·a^{-1}–46.85 kg/ha·a^{-1}, with an average of 8.04 kg/ha·a^{-1} (Wang et al., 2020). According to the research by Smil (1999), the nitrogen fixation factors differ with different crops; for instance, that of rice is 20–50 kg/ha·a^{-1} and that of wheat, corn, etc., is 5–20 kg/ha·a^{-1} (SMIL, 1999). In this research, the biological nitrogen fixation in the cultivated land in the irrigation area is 10 kg/ha·a^{-1}.

3.1.4 Crop nitrogen uptake per unit area per year (O_1)

The nitrogen uptake by rice plants is mainly from the nitrogen contained in chemical fertilizers, and the application of fertilizers in rice paddy fields contributes to increased yield. Nitrogen absorption per unit area of planting land (O_1) can be calculated based on the yield increase. The annual total nitrogen absorption is equal to the product of the increase in fertilizer yield and the sum of the nitrogen content ratios of grains and stems, where the increase in fertilizer yield is equal to the actual grain yield minus the base soil fertility yield.

Yield contributed by basic soil fertility refers to the grain yield per hectare harvested by traditional farming practices without the use of chemical fertilizers. Referring to the research by Li et al. (2022), the yield contributed by basic soil fertility of grain crops (represented by rice, wheat, and maize) in the Ningxia irrigation area is 4,167 kg/ha·a^{-1}; the grain nitrogen content ratio refers to the ratio of nitrogen content of harvested grains to the total weight of grains, which is 0.0369; the stem/grain nitrogen content ratio refers to the ratio of stem and leaf nitrogen content to grain nitrogen content of mature crops, which is taken as 0.5329 in this paper. From 2010 to 2022, the annual nitrogen uptake per unit area of crops in Ningxia irrigation districts decreased from 240.24 kg/ha·a^{-1}–219.81 kg/ha·a^{-1}, as detailed in Table 3.

3.1.5 Amount of N infiltrated into groundwater per unit area per year (O_3)

The nitrogen contents in water infiltration are different at different nitrogen application rates: when the nitrogen application rates are 120 kg/ha, 240 kg/ha, and 360 kg/ha, respectively, the nitrogen contents in water infiltration are approximately 13.87%, 16.32%, and 19.28%, respectively (Stephan and Endreny, 2016). The annual nitrogen input (nitrogen application rate) in this research is close to 360 kg/ha. Therefore, the nitrogen content in water infiltration is selected to be 19.28%.

3.1.6 Annual TN loss via runoff per unit area (O_4)

As the precipitation is small and the concentration of phosphorus and nitrogen in rainwater is low in the irrigation area, they basically have no impact on the TN and TP pollutant loads in agricultural drainage water. Therefore, the nitrogen pollutant load of rainfall input is not considered in this research. By balancing Equation (1), the annual total nitrogen loss per unit area from runoff in the Ningxia irrigation area was determined to be 26.85 kg/ha·a^{-1}, as detailed in Table 4.

3.2 Estimation of correction factors for return flow pollution load in irrigation district farmland

3.2.1 Irrigation impact factor

By analyzing the correlation between irrigation amount and agricultural non-point source pollutant load in the irrigation area, the relationship function between them is established, which will be

TABLE 4 Calculation results of the TN export coefficient of farmland planting (unit:kg/ha·a^{-1}).

Year	Annual nitrogen input (I_1)	Annual deposition Annual deposition net value (E_2)	Nitrogen fixation by farmland	Crop absorption (O_1)	Infiltration loss (O_3)	Export coefficient (O_4)
2010	311.57	0.1	10	240.34	50.85	30.48
2011	311.97	0.1	10	241.08	50.91	30.08
2012	309.29	0.1	10	242.66	50.48	26.25
2013	325.47	0.1	10	238.7	53.12	43.75
2014	313.08	0.1	10	212.45	51.09	59.64
2015	300.17	0.1	10	226.54	48.99	34.74
2016	294.66	0.1	10	239.1	48.09	17.57
2017	321.67	0.1	10	244.58	52.50	34.69
2018	286.82	0.1	10	246.85	46.81	3.26
2019	290.2	0.1	10	222.18	47.36	30.76
2020	280.82	0.1	10	223.71	45.83	21.38
2021	266.07	0.1	10	220.43	43.42	12.32
2022	255.6	0.1	10	219.81	41.71	4.18
Average	297.49	0.10	10	232.19	48.55	26.85

used to calculate the irrigation impact factor. The annual pollutant load and the annual non-point source irrigation amount are expressed in the functional expression, as shown below:

$$M_i = f(R_i) \quad (5)$$

where M_i presents the pollutant load exported by the irrigation area in the ith year, kg/a; and R_i presents the irrigation amount of the irrigation area in the ith year, m^3.

The model is mainly used to predict the multi-year average load of non-point source pollution in the watershed. Therefore, the multi-year average pollutant load in the irrigation area can be calculated by using the following equation:

$$\bar{M} = f(\bar{R}) \quad (6)$$

where $\bar{M}$ presents the average pollutant load in the irrigation area, kg/a; and $\bar{R}$ presents the average irrigation amount in the irrigation area, m^3.

Based on the pollutant load exported by the irrigation area and the average pollutant load, the irrigation impact factor (α) can be obtained:

$$\alpha = M_i/\bar{M} \quad (7)$$

Based on the equation including the agricultural irrigation amount and non-point source TN load in Ningxia obtained in the research by Yang Shujing et al., the TN load is calculated (He et al., 2022):

$$y = 13017e^{0.0073x} \quad (8)$$

where y is the TN load, t; and x is the irrigation amount, 10^8 m^3.

Substituting the irrigation amounts from 2010 to 2023, the annual non-point source TN load in the irrigation area can be calculated; by substituting the annual average irrigation amount of 6.0404 billion m^2, the multi-year average of non-point source TN load in the irrigation area can be obtained. In this way, the irrigation impact factors in the Ningxia irrigation area from 2010 to 2023 can be calculated, with the results shown in Table 5.

3.2.2 Precipitation impact factor

The impact of the spatial distribution of precipitation on non-point source pollution mainly refers to the difference in non-point source pollution caused by different precipitation in different regions in a certain year. The precipitation impact factor (β) is expressed as follows:

$$\beta = \frac{R_j}{\bar{R}} \quad (9)$$

where, β presents the precipitation impact factor; R_j presents the precipitation amount of the watershed in the jth year, mm; and $\bar{R}$ presents the average precipitation amount in the whole watershed, mm.

The monthly precipitation amounts in the Ningxia irrigation area (provided by Yongning County Meteorological Station) in a whole year are shown in Table 6.

It is shown in Table 3 that the precipitation amounts in June, July, and August in Ningxia irrigation area are larger than those in other months of the same year. The field-steeping period and the effective tillering period in the irrigation area are May and June, and the jointing and booting period are July and August, respectively. It is seen that the precipitation amount accounts for more than 70% of the whole year during the growth of rice. Therefore, precipitation will have a certain impact on agricultural drainage water and pollutant load. The average precipitation amount in the Ningxia irrigation area from 2010 to 2022 is 195.45 mm. Based on the precipitation amounts from 2010 to

TABLE 5 Irrigation impact factors in the Ningxia irrigation area from 2010 to 2023.

Year	Irrigation amount/10^8 m^3	Non-point source TN load/t	TN irrigation impact factor
2010	66.402	21136.28	1.045
2011	66.980	21225.65	1.049
2012	62.431	20532.31	1.015
2013	65.040	20927.13	1.034
2014	60.962	20313.35	1.004
2015	61.560	20402.21	1.008
2016	55.949	19583.42	0.968
2017	56.356	19641.74	0.971
2018	56.254	19627.15	0.970
2019	59.118	20041.70	0.991
2020	58.131	19897.83	0.984
2021	55.668	19543.37	0.966
2022	55.410	19506.50	0.964
2023	55.362	19499.50	0.964

TABLE 6 Monthly precipitation amounts in the Ningxia irrigation area in a whole year.

Year	Jan.	Feb.	Mar.	Apr.	May	Jun.	Jul.	Aug.	Sep.	Oct.	Nov.	Dec.	Whole year
2010	0	11.7	1.9	9.9	35.7	37	17	3.4	42.9	9.4	0	0	168.9
2011	1.8	0.2	0	4.3	29	1	16	56.2	40.7	13.4	26.1	0	188.7
2012	2.7	0	1.2	28.2	12.4	42.9	137.1	21	44	4.8	0.5	0.3	295.1
2013	0.7	0	0	5.5	44.5	26.3	30.5	16.9	21.3	2.6	0	0	148.3
2014	0	4.7	0	30.8	0.8	46.7	21.1	57	13.1	16.6	5.3	0	196.1
2015	0.3	0.1	0	28.7	8.6	5.2	7.8	16.1	76.1	17.6	25.4	9.6	195.5
2016	0.1	8.9	22.2	16.2	26.5	8.8	71.6	52.8	6.3	28.5	0	0	241.9
2017	0	9.3	18.1	4.2	6.2	36	41	39.8	14.1	36.3	0	0.3	205.3
2018	4	0	2.5	29.1	20.5	2.9	73.7	79.1	34.1	6.8	1.7	1.9	256.3
2019	1.1	0	0	9.1	11.4	100.6	5.3	4.3	28.8	14.5	1.9	0.2	177.2
2020	1.2	0	0	0.6	8.6	42.1	17.6	71.3	27.7	0.9	7	1	178
2021	0	3.3	25.5	13.6	15.4	12.1	0.9	12.3	50.1	6.2	14.5	0	153.1
2022	0.2	5.6	1.3	3.2	5.5	21.9	37.7	38.1	6.6	11.9	4.4	0	136.4

2022 provided in the table, the precipitation impact factor can be calculated. See Table 7 below for details.

3.3 Discussion

3.3.1 Estimation of TN total pollution load in agricultural drainage water

Previous scholars, when improving the ECM, often incorporated rainfall and topographic factors to account for land use diversity and terrain complexity. However, this study considers that the Ningxia irrigation district is a plain area with a flat terrain, and that the primary crop generating farmland drainage water is rice. Given the significant impact of irrigation volume on pollutant export in farmland drainage, this study employed irrigation and rainfall factors as correction factors for the ECM. This approach better reflects the actual conditions of pollution export from farmland drainage in the Ningxia irrigation district. Using the improved ECM and rice cultivation area data, the estimated multi-year average TN pollution load in the Ningxia irrigation district was 2064.95 t (see Table 8 for details). The corrected multi-year average TN pollution load increased by 133.76 t compared to the uncorrected value,

TABLE 7 Precipitation impact factors in the Ningxia irrigation area from 2010 to 2022.

Year	Precipitation amount/mm	Precipitation impact factor
2010	168.9	0.86
2011	188.7	0.97
2012	295.1	1.51
2013	148.3	0.76
2014	196.1	1.00
2015	195.5	1.00
2016	241.9	1.24
2017	205.3	1.05
2018	256.3	1.31
2019	177.2	0.91
2020	178	0.91
2021	153.1	0.78
2022	136.4	0.70

TABLE 8 Total pollutant load of TN in the Ningxia irrigation area.

Year	Export coefficient/kg/ha· a^{-1}	Rice planting area/ha	Irrigation impact factor	Precipitation impact factor	Corrected TN pollutant total load/t
2010	30.48	83158.51	1.045	0.86	2,277.91
2011	30.08	83942.70	1.049	0.97	2,569.26
2012	26.25	84339.48	1.015	1.51	3,393.15
2013	43.75	82144.87	1.034	0.76	2,824.18
2014	59.64	78044.43	1.004	1.00	4,673.19
2015	34.74	74343.49	1.008	1.00	2,603.35
2016	17.57	80865.14	0.968	1.24	1705.42
2017	34.69	81083.38	0.971	1.05	2,867.77
2018	3.26	78009.61	0.97	1.31	323.15
2019	30.76	68056.58	0.991	0.91	1887.87
2020	21.38	60814.95	0.984	0.91	1164.27
2021	12.32	50839.16	0.966	0.78	471.93
2022	4.18	29374.52	0.964	0.70	82.86
Average	26.85	71924.37	—	—	2064.95

representing an increase of 6.48%. This result is relatively close to the 5% reduction in relative error for TN load estimation using an improved model reported by Shu-jing et al. (2009). Both the irrigation and precipitation correction factors are driving factors influencing pollution loads in farmland drainage within irrigation districts. Although irrigation water volume and precipitation may decrease, the concentration of pollutants in farmland drainage may increase. Consequently, the pollution load does not decrease proportionally with reduced water volumes but instead shows a slight increase. This further demonstrates that the improved ECM more accurately approximates real-world conditions.

3.3.2 Temporal variation characteristics of TN pollution load in agricultural drainage water from irrigation districts

From 2010 to 2022, the TN output load from the irrigation district in Ningxia experienced significant fluctuations. It initially

FIGURE 3
Total TN export load in the Ningxia irrigation area from 2010 to 2022.

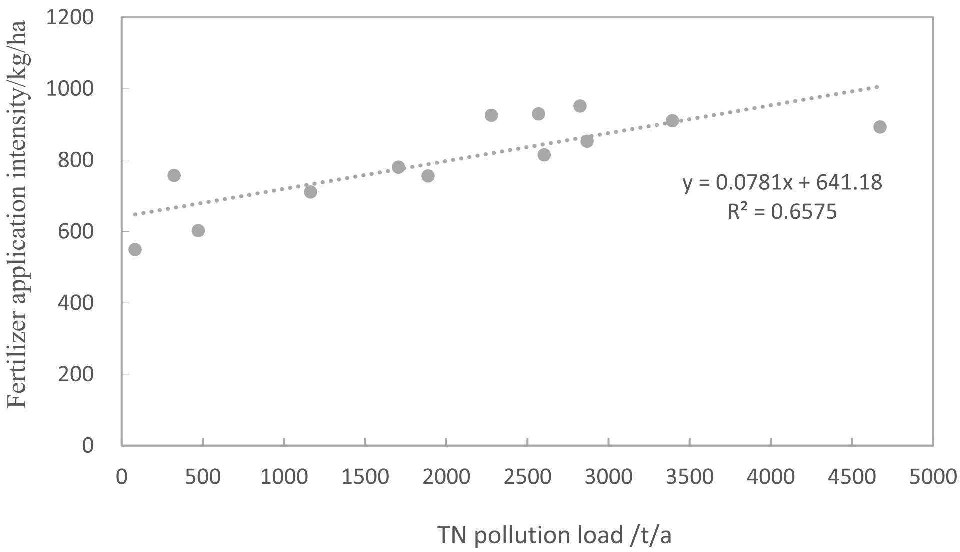

FIGURE 4
Fertilizer application intensity scatter plot.

increased from 2,277.91t/a in 2010, reaching a peak of 4,673.19 t/a in 2014, followed by a substantial decline to a minimum of 82.86 t/a in 2022. Overall, the trend was characterized by fluctuation with a general downward trajectory. For detailed information, please refer to Figure 3.

The TN pollution load in farmland drainage within the irrigation district is influenced by several factors, including nitrogen fertilizer application intensity, planting area, irrigation water volume, and rainfall. The calculated correlation coefficients are 0.81, 0.67, 0.57, and 0.25, respectively. These results indicate that nitrogen fertilizer application intensity and planting area are the primary contributing factors to TN pollution load in farmland drainage. Detailed trend analyses are presented in Figures 4–7. In recent years, with the total control of water resources in the Yellow River and the contradiction between water supply and demand in Ningxia, the planting structure has undergone significant changes. The area of rice planting has been on a downward trend since 2017, especially in 2022, when the area of rice planting was relatively large, a 64% decrease compared to that in 2010. The irrigation district in Ningxia is a semi-arid area with low rainfall. The average rainfall from 2010 to 2022 was less than 200 mm, and the irrigated water volume is relatively small. The impact on the total nitrogen output load of the irrigation district in Ningxia is relatively minimal.

10.3389/fenvs.2025.1626677

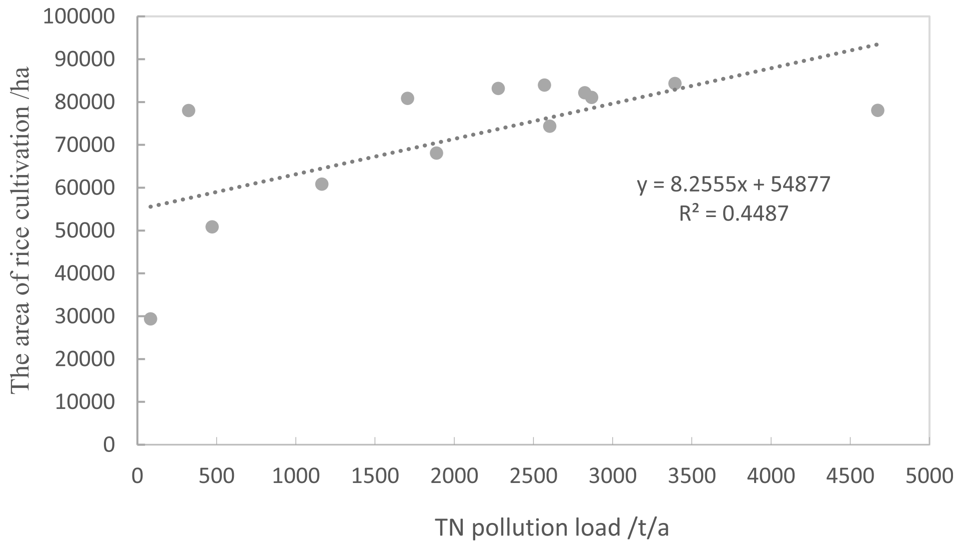

FIGURE 5
The area of the rice cultivation scatter plot.

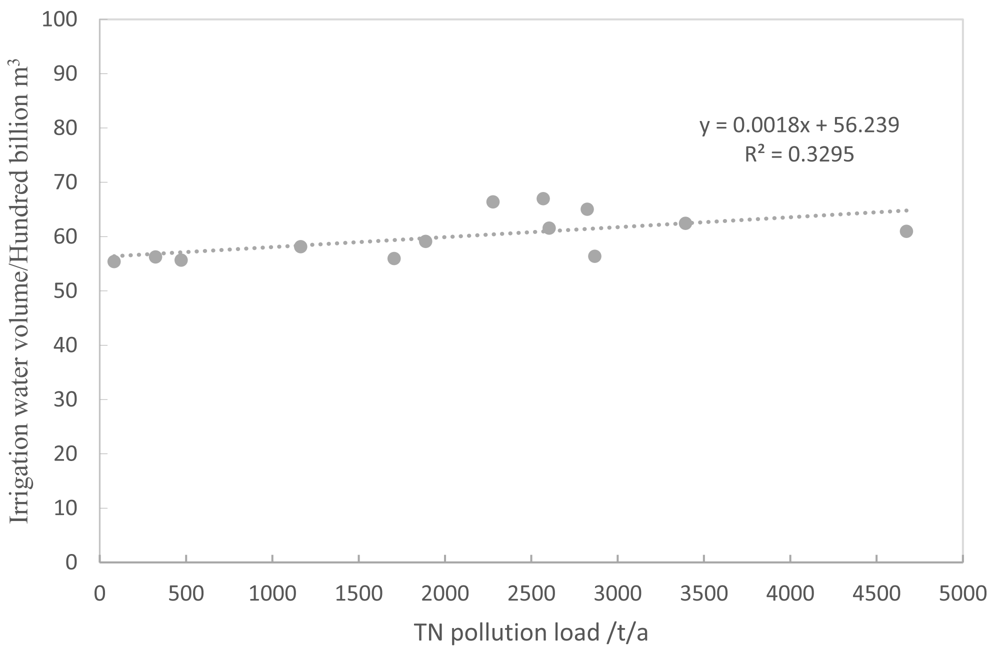

FIGURE 6
Irrigation water volume scatter plot.

3.3.3 The spatial variation characteristics of TN pollution load in agricultural drainage water within irrigation districts

The TN total pollution load in different districts and counties of the Ningxia irrigation area varies considerably, influenced by factors such as rice cultivation area, fertilizer application intensity, irrigation volume, and precipitation in the region. The distribution of the TN pollution load in 2010, 2015, and 2020 is shown in Figure 8.

Based on the distribution of total pollution load, the irrigation areas of Ningxia can be categorized into zones of high, moderate, and low agricultural return flow pollution load. Efforts should be intensified to prevent non-point source pollution in high-load zones through a "source-migration-sink" approach, thereby reducing the impact of agricultural return flow on water pollution in the Yellow River Basin.

3.3.3.1 High-pollution load zones (total load ≥150 t/a)

In 2010, high-pollution load zones were distributed across 7 regions: Xingqing District, Yongning County, Helan County, Lingwu City, Pingluo County, Qingtongxia City, and Shapotou

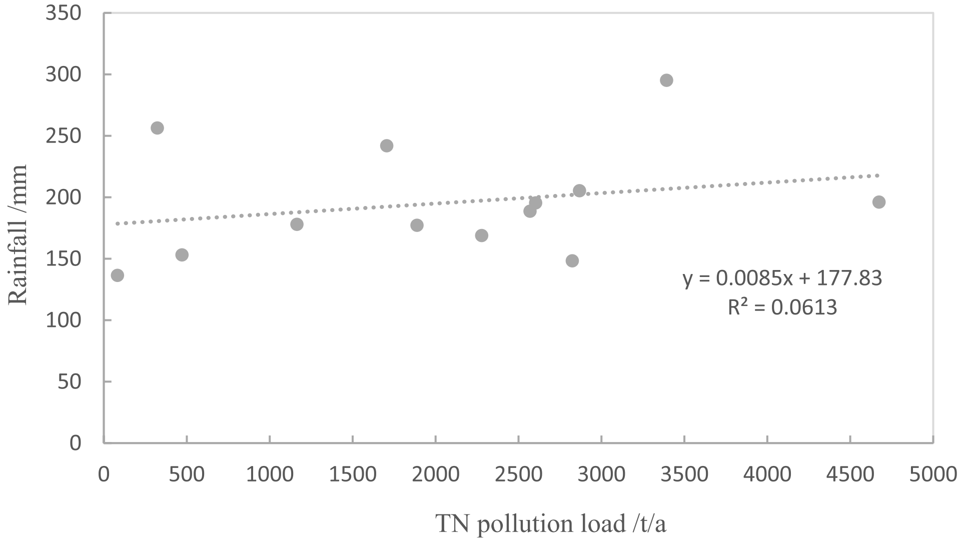

FIGURE 7
Rainfall scatter plot.

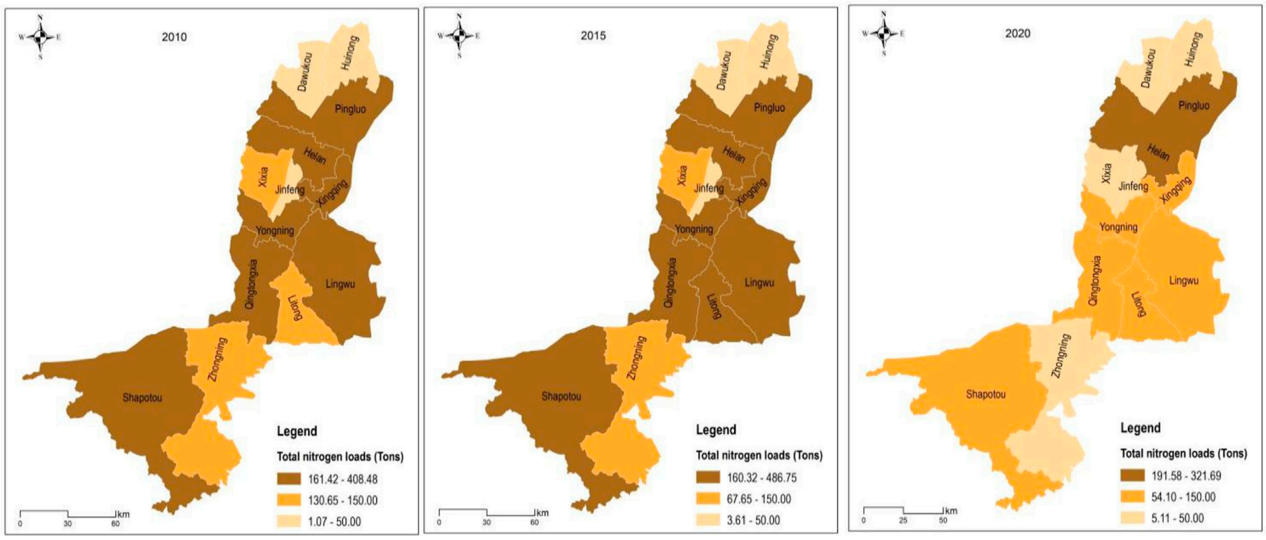

FIGURE 8
Distribution of the TN total pollution load in the Ningxia irrigation area.

District; in 2015, distributed across 8 regions: Xingqing District, Yongning County, Helan County, Lingwu City, Pingluo County, Litong District, Qingtongxia City, and Shapotou District; and in 2020, distributed across 2 regions: Helan County and Pingluo County. Overall, the number of high-load zones showed an initial increase followed by a decrease.

3.3.3.2 Moderate-pollution load zones (total load: 50 t/a–150 t/a)

In 2010, moderate-pollution load zones were distributed across 3 regions: Xixia District, Litong District, and Zhongning County; in 2015, distributed across 2 regions: Xixia District and Zhongning County; and in 2020, distributed across 6 regions: Xingqing District, Yongning County, Lingwu City, Litong District, Qingtongxia City, and Shapotou District.

3.3.3.3 Low-pollution load zones (total load ≤50 t/a)

In 2010, low-pollution load zones were distributed across 3 regions: Jinfeng District, Dawukou District, and Huinong District; in 2015, distributed across 3 regions: Jinfeng District, Dawukou District, and Huinong District; and in 2020, distributed across 5 regions: Xixia District, Jinfeng District, Dawukou District, Huinong District, and Zhongning County.

4 Conclusions and prospects

4.1 Conclusion

Based on the estimation of TN pollution load from agricultural drainage water in the Ningxia irrigation area and the study of its spatiotemporal variation characteristics, the following main conclusions were drawn.

1) Using the improved ECM, the multi-year average values of the TN export coefficient and total export load from farmland drainage in the Ningxia irrigation area during 2010–2022 were estimated as 26.85 kg/ha·a^{-1} and 2064.95 t/a, respectively. The improved total export load increased by 6.48% compared to the original ECM.
2) The TN total pollution load from agricultural drainage water in the Ningxia irrigation area showed an overall downward trend from 2010 to 2022, with the lowest load recorded in 2022 (82.86 t/a). The primary reason for this change was the dramatic decline in rice cultivation area caused by significant shifts in crop structure.
3) Spatial distribution characteristics of the TN total pollution load were similar across the three periods (2010, 2015, and 2022), exhibiting distinct spatial heterogeneity. The load was unevenly distributed overall, with localized concentration. Areas with high pollution loads showed a trend of initially increasing and then decreasing. Key areas requiring management were mainly distributed in Pingluo County, Helan County, and Lingwu City.

4.2 Prospects

The mechanism of agricultural drainage pollution export in irrigation districts is complex and highly dependent on regional characteristics and input data accuracy. Although this paper adopts an improved ECM that comprehensively considers influencing factors such as meteorology, hydrology, and crop cultivation—identifying irrigation as the primary factor affecting pollution load—it develops a non-point source pollution load estimation model suitable for large- and medium-sized basins. This model is particularly adapted to areas with insufficient hydrological and water quality monitoring data and relatively weak research foundations, such as the Ningxia irrigation district. But the improved model itself remains largely empirical or semi-empirical. Consequently, it struggles to fully capture complex biogeochemical processes and lacks detailed characterization of nitrogen loads under extreme conditions, including heavy rainfall, abnormally high/low temperatures, sudden irrigation events, or fertilization errors. Furthermore, the scarcity of fine-scale data, such as farmland microclimate, effluent water quality, and actual fertilization/irrigation practices, impedes the model's sensitivity analysis and uncertainty quantification.

To comprehensively address the complexity inherent in agricultural drainage water pollution processes, future studies could leverage the efficiency and macroscopic advantages of the ECM to enhance the detailed characterization of key mechanisms when integrated with process-based models. For instance, the improved ECM could be coupled with distributed hydrological models or biogeochemical models possessing a stronger physical foundation. To mitigate data limitations, remote sensing technologies (e.g., hyperspectral, thermal infrared, and radar) can be widely employed to invert key parameters such as crop growth status, soil moisture, land surface temperature, and evapotranspiration rates, thereby compensating for the scarcity of ground-based observations. Ultimately, an improved ECM methodological framework and associated key parameter system, specifically tailored for arid and semi-arid irrigation regions, can be developed and refined. This will provide valuable reference for quantifying and managing agricultural drainage water pollution in analogous study areas. In addition, drawing upon the full life cycle theory, it is possible to examine the influence of factors such as climate change on the dynamic load of nitrogen in various forms, thereby enabling an analysis of the spatiotemporal distribution characteristics of nitrogen pollution loads (Ugural et al., 2024).

Data availability statement

The original contributions presented in the study are included in the article/supplementary material; further inquiries can be directed to the corresponding author.

Author contributions

LY: Conceptualization, Data curation, Investigation, Methodology, Project administration, Writing – original draft, Writing – review and editing. YO: Formal Analysis, Methodology, Writing – review and editing, Data curation. YY: Data curation, Validation, Visualization, Writing – original draft.

Funding

The author(s) declare that financial support was received for the research and/or publication of this article. This research was funded by the Fundamental Research Funds for the Central Universities (Grant No.20240222).

Conflict of interest

The authors declare that the research was conducted in the absence of any commercial or financial relationships that could be construed as a potential conflict of interest.

Generative AI statement

The author(s) declare that no Generative AI was used in the creation of this manuscript.

Publisher's note

All claims expressed in this article are solely those of the authors and do not necessarily represent those of their affiliated organizations, or those of the publisher, the editors, and the reviewers. Any product that may be evaluated in this article, or claim that may be made by its manufacturer, is not guaranteed or endorsed by the publisher.

References

Chaofan, L., Beibei, Z., Chen, X., and Shan, L. (2020). Application and progress of DRAINMOD model in agricultural drainage system. *J. Irrigation Drainage* 39 (1), 101–106+112.

Chen, W., Wan, Y., Guo, Y., Ji, G., and Shi, L. (2025). Predicting Non-point source pollution in Henan Province using the diffuse pollution estimation with remote sensing model with enhanced sensitivity analysis. *Appl. Sci.* 15, 2261. doi:10.3390/app15052261

Geng, R. Z., Wang, X. Y., Jiao, S., Meng, F. D., and Duan, S. H. (2013). Application of improved export coefficient model in estimating non-point source nutrient load from miyun reservoir watersheds. *Acta Sci. Circumstantiae* 33 (5), 1484–1492.

Girolamo, D. M. A., Spanò, M., D'Ambrosio, E., Giovanni, F., and Francesco, G. (2019). Developing a nitrogen load apportionment tool: theory and application. *Agric. Water Manag.*, 226105806–105806.

Gou, T., Pei, D. F., Liang, R. C., She, L., Yang, J., and Ma, Q. L. (2023). Analysis of nitrogen and phosphorus emission characteristics from agricultural non-point sources based on the export coefficient method. *China Environ. Sci.* 43 (12), 6539–6550.

Haiyang, C., Yanguo, T., and Jinsheng, W. (2013). Load estimation and source apportionment of nonpoint source nitrogen and phosphorus based on integrated application of SLURP model, ECM, and RUSLE: a case study in the jinjiang river, China. *Environ. Monit. Assess.* 185 (2), 2009–2021. doi:10.1007/s10661-012-2684-z

HuaLin, L., ShouHong, Z., PeiDan, Y., Zhuoyuan, S., Chenxin, X., and Jianjun, Z. (2023). Estimation and critical source area identification of non-point source pollution based on improved export coefficient models: a case study of the upper beiyun river basin. *Environ. Sci.* 44 (11), 6194–6204.

Jia, Z. (2024). *Simulation study on legacy effect of watershed nitrogen non-point source pollution and its spatial distribution characteristics*. Hangzhou, China: Zhejiang University.

Li, T., Niu, Y., Pang, J., Geng, S., Wang, Y., Li, J., et al. (2024). Temporal and spatial characteristics of agricultural non-point source pollution in Hebei Province from 2000 to 2021. *Front. Environ. Sci.* 12, 121439806–1439806. doi:10.3389/fenvs.2024.1439806

Li, M. B., Zhou, B. J., Hu, K. X., and Wang, J. I. (2025). Estimation of non-point source nitrogen and phosphorus loads using an improved export coefficient modeling approach. *J. China Environ. Sci.* 45 (6) 3321–3330.

Li, Y., Zhou, B., Liu, H. L., Wang, Y. X., Xing, M. N., and Ji, M. (2018). Analysis of the non oint source polu-tion load from the storm runoff and itscontrol strategy for haihe river Trunkstream.Tianjin. *J. Saf. Environ.* 18 (01), 230–235.

Liang, T., Tong, Y. A., Lin, W., Qiao, L., Liu, X. J., Bai, S. C., et al. (2014). Spatial-temporal variability of dry and wet deposition of atmospheric nitrogen in differentecological regions of Shaanxi. *Acta Ecol. sin.* 34 (3), 738–745. doi:10.5846/stxb201211011517

Liang, Y. Y., Song, Z. H., Li, L. J., Bai, G. J., Lu, W., and Liu, P. (2019). Characteristics of dry and wet deposition of atmospheric nitrogen farmland area in suburb of taiyuan city. *J. Shanxi Agric. Sci.* 47 (11), 2003–2008.

Liu, R., Yu, W., Shi, J., Wang, J., Xu, F., and Shen, Z. (2017). Development of regional pollution export coefficients based on artificial rainfall experiments and its application in north China. *Int. J. Environ. Sci. Technol.* 14 (4), 823–832. doi:10.1007/s13762-016-1187-9

Liu, X. T., Sun, Y., Zhao, Y., Luo, J. H., Ma, Y., Zhang, T. P., et al. (2025). Response characteristics of nitrogen concentration in farmland and irrigation ditches in the yellow river water diversion irrigation area of Ningxia. *J. Agro-Environment Sci.* 44 (05): 1343–1352. Available online at: http://kns.cnki.net/kcms/detail/12.1347.S.20241016.1014.004.html.

Lu, J. Z., Chen, X. L., Xiao, J. J., Yu, J. X., and Liu, H. (2012). Application of improved export coefficient method in estimation of agricultural source pollution. *J. Huazhong Normal Univ. Sci.* 46 (3), 373–378.

Lu, Y., Tong, B., Wang, Le, and Han, X. (2024). Analysis and research on the current situation of non-point source pollution in typical drainage ditches of Ningxia in the yellow river irrigation area. *Environ. Sci. Manag.* 49 (09), 118–122.

Meng, X. J., Wang, X. J., Ju, N., and Ge, G. H. (2024). Spatio-temporal characteristics and pollution sources of agricultural non-point source pollution in Shaanxi Province. *Hubei Agric. Sci.* 63 (02), 224–231.

Pei, W., Lei, Q. L., Li, Y., Zhao, Y., Liu, X. T., and Tian, L. F. (2024). Spatiotemporal distributions of water quality of drainage ditches and its pollution source analysis from 2014 to 2019 in qingtongxia irrigation district. *Chin. J. Agric. Resour. Regional Plan.* 45 (03), 36–48.

Schlesinger, W. H., and Bernhardt, E. S. (2013). *Biogeochemistry: an analysis of global change*. 3rd ed. Academic Press.

Yang, S. J., Zhang, A. P., Yang, Z. L., and Yang, S. Q. (2009). Agricultural Non-point source pollution in Ningxia irrigation districtand preliminary study of load estimation methods. *Sci. Agric. Sin.* 42 (11), 3947–3955.

Smil, V. (1999). Nitrogen in crop production:an account of global flows. *Glob. Biogeochem. Cycles* 13 (2), 647–662. doi:10.1029/1999gb900015

Stephan, A. E., and Endreny, A. T. (2016). Weighting nitrogen and phosphorus pixel pollutant loads to represent runoff and buffering likelihoods. *JAWRA J. Am. Water Resour. Assoc.* 52 (2), 336–349. doi:10.1111/1752-1688.12390

Ugural, M. N., Ozyilmaz, M. R., and Burgan, H. I. (2024). Life cycle assessment analysis based on material selection in sustainable airport buildings. *Buildings* 14 (9), 2728. doi:10.3390/buildings14092728

Xiaoyuan, Z., Zhongwei, Z., Xiaojie, L., Zhang, Q., Wang, L., Chen, H., et al. (2023). Application of modified export coefficient model to estimate nitrogen and phosphorus pollutants from agricultural non-point source. *J. Geogr. Sci.* 33 (10), 2094–2112. doi:10.1007/s11442-023-2167-x

Wang, X., Yao, Y., Xu, M. J., and Zhuang, S. Y. (2020). Spatial differentiation characteristics of biological nitrogen fixation in surface soil of paddy fields in yixing city. *Soil* 52 (03), 618–624.

Xinyu, Z., Liangjun, F., and Liu, C. (2007). Analysis and simulation of groundwater level changes in qingtongxia yinbei irrigation area. *Agric. Res. Arid Regions* 25 (2), 120–123.

Yuanzhe, W., Chunlin, H., Min, F., Yao, J., Zhou, L., Cai, C., et al. (2023). Spatial and temporal distribution characteristics of typical pollution loads based on SWAT model across tuojiang river watershed located in Sichuan Province, southwest of China. *Environ. Monit. Assess.* 195 (7), 865. doi:10.1007/s10661-023-11481-6

Li, Y. H., Wang, H. Y., Cui, Z. L., Ying, H., Qu, X. L., and Zhang, J. D. (2022). Spatial-temporal variation of cultivated land soil basic productivity for main food crops in China. *Sci. Agric. Sin.* 55 (20), 3960–3969.

He, Y., Yang, A. J., Chen, W. J., Guo, Y., Feng, Y. H., and Song, X. (2022). Agricultural non-point source pollution load and distribution characteristics in a typical watershed of the southwest karst Mountain area. *Res. Soil Water Conservation* 29 (01), 148–152.

Zhang, S., Zhang, L., Meng, Q., Wang, C., Ma, J., Li, H., et al. (2024). Evaluating agricultural non-point source pollution with high-resolution remote sensing technology and SWAT model: a case study in Ningxia yellow river irrigation district, China. *Ecol. Indic.* 166, 166112578–112578. doi:10.1016/j.ecolind.2024.112578

Hu, Z., Ao, T. Q., Li, M. R., Hu, F. C., and Liu, L. X. (2019). Analyzing Non-point pollution in areas with scarce data using modified output-coefficient model. *J. Irrigation Drainage* 38 (02), 108–114.